Chinese Chemical Letters 32 (2021) 1385–1389

Contents lists available at ScienceDirect

Chinese Chemical Letters

journal homepage: www.elsevier.com/locate/cclet

Communication

Host-guest co-assembly triggered turn-on and ratiometric sensing of berberine and its detoxicating

Chuanfeng Liu[a], Zhixin Li[a], Hai Yu[a], Naibin Cui[a], Xiaoyu Liao[b], Haibin Zhang[a], Zhengning Shu[a], Peng Yang[a,*]

[a] Wuya College of Innovation, Shenyang Pharmaceutical University, Shenyang 110016, China
[b] School of Traditional Chinese Materia Medica, Shenyang Pharmaceutical University, Shenyang 110016, China

ARTICLE INFO

Article history:
Received 4 August 2020
Received in revised form 16 October 2020
Accepted 30 October 2020
Available online 2 November 2020

Keywords:
Recognition
Macrocycle
Host-guest
Sensor
Carbazole

ABSTRACT

Fluorescent sensing for specific detection of berberine is an important issue in view of its potential jeopardization to food safety and human health, but remains less investigated. To the best of our knowledge, there is no fluorescence turn-on and ratiometric sensors available for specific detection of berberine. In this study, calix[4]carbazole (**3**) has been synthesized and its property of recognizing berberine has been evaluated by UV–vis, fluorescence, NMR, DLS and TEM techniques. The results show that **3** selectively recognizes berberine among the tested drugs and detects it with turn-on and ratiometric fluorescence due to their co-assembly nature. Moreover, **3** is not only low toxic and can reduce toxicity of berberine to human normal liver L02 cell, but also can release berberine to tumor HepG2 cells at acid micro-environment. It therefore holds a great potential for further exploration

Berberine, a naturally occurring isoquinoline alkaloid, is clinically used to treat bacterial diarrhea [1,2]. Recently, its diversified potency against various diseases, such as antimicrobial, antitumor activity as well as the ability of ameliorating metabolic disorders, has also been found [3–7]. To cure these diseases, a certain plasma concentration is required. However, animal studies indicate that the exorbitant concentration of berberine may be fatal to human health [8]. On the other hand, the extensive use of berberine in foods, animal husbandry as well as breeding industry in recent years has caused much concern due to its potential jeopardization to food safety [9–11]. Therefore, both clinical therapy and food stuff require a safety concentration range of berberine. In view of the importance of detection of berberine, several strategies including chromatographic, electrochemical and spectral analyses have been proposed and lots of efforts have been made [12–21]. Among them, the fluorescent detection is a sensitive, rapid, low cost, easily managed method and especially valuable for biological systems. Unfortunately, fluorescent sensors for berberine remain less reported [22]. To the best of our knowledge, there is no fluorescence turn-on and ratiometric sensors available for specific detection of berberine.

A sensor is usually composed of both a fluorophore and a receptor, the latter of which determines its specificity. Various macrocycles including cyclodextrins, cucurbiturils as well as calixarenes are reported to be able to serve as receptors of berberine [23–35]. But neither the specificity nor the sensing ability is satisfactory so far. Moreover, in order to gain a specific macrocyclic sensor, sophisticated synthetic works are usually required and sometimes may be challenging.

Our group has ever reported a novel series of carbazole-based macrocyles in 2016, named as calix[*n*]carbazoles [36]. Due to the fluorescent properties of its carbazolyl moiety, these macrocycles are inherent sensors without being conjugated with additional fluorophores. Our previous works show that differently modified calix[*n*]carbazoles could be able to detect different guests [37–42]. Those results promote us to further explore its potential of serving as the sensor for berberine. Toward this end, we recently synthesized a calix[4]carbazole (**3**, Scheme 1) with the head group of thiophenecarboxylic acid and examined its property of sensing drugs. To our joy, this molecule is able to detect berberine selectively with fluorescence turn-on and ratiometric signals *via* Fluorescence Resonance Energy Transfer (FRET) mechanism, in which an excited state donor transfers its energy to a ground state acceptor through a certain long distance [43]. Moreover, this molecule is not only of low toxicity but also can reduce the toxicity of berberine toward human normal liver cell line L02 due to its pH-dependent drug-releasing nature. To the best of our knowledge,

* Corresponding author.
E-mail address: yangpeng@syphu.edu.cn (P. Yang).

https://doi.org/10.1016/j.cclet.2020.10.048
1001-8417/

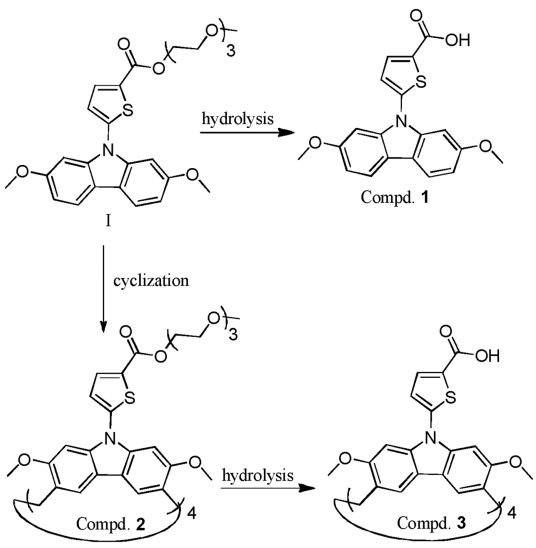

Scheme 1. The synthetic routes for target compound **3.**

this smart macrocycle represents the first fluorescent sensor capable of turn-on and ratiometric detecting berberine as well as detoxicating it. We herein report our findings.

Scheme 1 presents the synthetic route for the target compound **3**. In this study, 2-thiophenecarboxylic acid ester substituted carbazole, other than acetic acid ester substituted one in the previous work [36–42], is used as the monomer (**I**) to construct the macrocycle. We propose that such a rigid spacer between acid unit and carbazolyl moiety may favor its molecular recognition property. The methoxytriglycol acetate side chain is used to expand the solubility of the target compound in various solvents and in order to facilitate the purification [36]. The synthesis of **I** follows the literature [44]. The cyclization reaction is carried out based on our previously developed procedure [36]. As usual, the cyclization gives two major products of both the cyclotrimer and the cyclotetramer (**2**). The different numbers between calix[3]-carbazole and calix[4]carbazole could be clarified by the differences of their ^{1}H NMR, MS as well as their TLC patterns (Schemes S1 and S2 in Supporting information). **2** is hydrolyzed under basic condition to give the target compound **3**. **I** is hydrolyzed to give **1**, used as the control in this work. All of these compounds are fully characterized (Figs. S1–S21 in Supporting information).

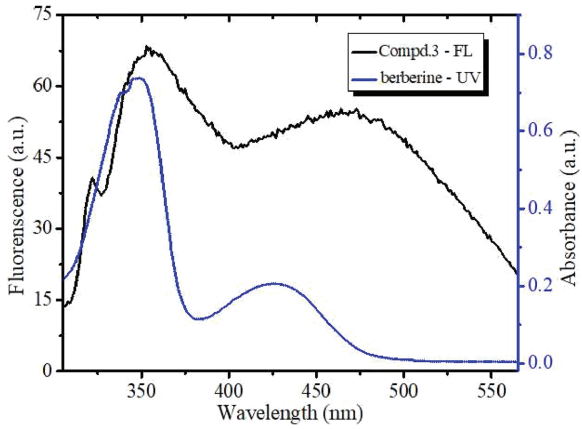

Fig. 1. Fluorescence spectrum of **3** (λ_{ex} = 290 nm) and UV–vis spectrum of berberine in deionized water containing 40% DMSO.

One of the merits of FRET sensors is that it can detect targets with turn-on and ratiometric fluorescence. But it takes place only when the acceptor can absorb the energy at the emission wavelength of the donor. To explore the possibility of **3** as a FRET sensor for berberine, we firstly examined their UV–vis and fluorescence spectra, which were shown in Fig. S22 (Supporting information). Fig. 1 shows both the fluorescence spectrum of **3** and UV–vis spectrum of berberine. It can be seen that the fluorescence of **3** at ~350 nm and ~465 nm is overlapped with the absorption bands of berberine at ~350 nm and ~420 nm. The emission spectrum of the donor (**3**) fully covers the absorption spectrum of the berberine acceptor. The spectral features make it possible that **3** could be able to act as the FRET sensor of berberine, as long as it could specifically interact with berberine.

With this idea in mind, we then recorded the fluorescence of **3** upon addition of berberine. Fig. 2a shows that upon addition of berberine, the emissions of **3** at both ~350 nm and ~465 nm drop gradually, whereas the fluorescent peak of berberine at ~545 nm increases gradually, a typical FRET spectral pattern. A distinct isoemission point at 507 nm is observed, an indicative of the specific host-guest binding. A calibration curve in Fig. 2b shows a good linear relationship between F_{545nm}/F_{465nm} and the concentration of berberine hydrochloride in the range of 2.25~30 μmol/L. The standard regression equation is $F_{545nm}/F_{465nm} = 0.6110 + 0.0220\ c$ ($R^2 = 0.9936$). This result indicates that **3** is able to ratiometrically detect berberine and the calculated limit of detection (LOD) is 9.35 nmol/L.

For comparison, we recorded the fluorescent spectra of the control compound **1** upon addition of berberine (Fig. S23 in Supporting information). It can be seen that the addition of berberine quenches the fluorescence of **1**. However, the emission peak of berberine at ~545 nm is not observed. In other words, FRET between **1** and berberine does not occur. This result indicates that the interaction between berberine and **1** is different from its binding pattern to **3**. Compared to **3**, **1** lacks a well-defined cavity so that it cannot encapsulate berberine. It interacts with berberine only through non-specific binding forces such as electronic static binding, π-π stacking as well as hydrophilic/hydrophobic binding.

In order to learn binding selectivity, we examined the fluorescence of **3** upon binding to some other analytes including various ions and drugs (Fig. S24 in Supporting information). The results are listed in Fig. 3 and Fig. S25 (Supporting information). It can be seen that these analytes do not change F_{545nm}/F_{465nm} of **3** as remarkably as berberine does, which indicates the berberine-specific sensing nature of **3**. In comparison with other analytes, F_{545nm}/F_{465nm} ratio of **3** upon binding to berberine is the highest, which indicates its excellent selectivity.

In order to gain insight of **3**-berberine binding mechanism, we firstly look back into the fluorescent spectrum of **3** in Fig. 1, in which two major peaks at ~350 nm and at ~465 nm are observed. Based on our previous knowledge, the fluorescence at ~350 nm

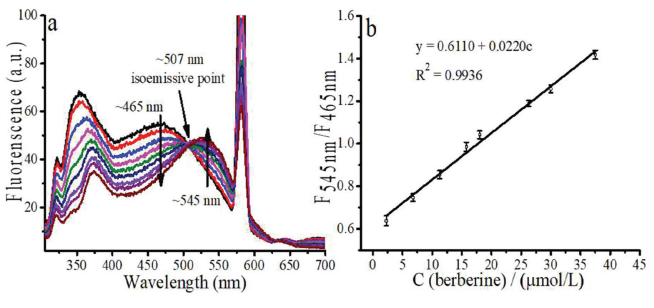

Fig. 2. (a) Fluorescence of **3** (10 μmol/L) upon addition of berberine (3, 9, 15, 21, 27, 35, 40, 50 μmol/L) in deionized water containing 40% DMSO (λ_{ex} = 290 nm). (b) Linear relationship between F_{545nm}/F_{465nm} with the concentration of berberine.

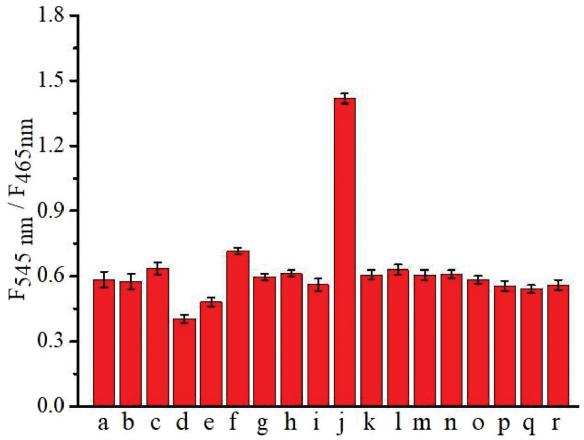

Fig. 3. $F_{545nm}/F_{465\ nm}$ of **3** (10 μmol/L) in the presence of various analytes (20 μmol/L) in deionized water containing 40% DMSO (λ_{ex} = 290 nm). (a) Cytarabine; (b) Taxol; (c) Artemisinine; (d) D-Tetrandrine; (e) Berbamine; (f) Demethyleneberberine; (g) Glutathione ; (h) D-Ribose; (i) Cytosine; (j) Berberine; (k) Ba^{2+}; (l) Ca^{2+}; (m) K^+; (n) Mg^{2+}; (o) Zn^{2+}; (p) COO^-; (q) I^- and (r) NO^-.

should be attributed to the monomer of 2,7-dimethoxylcarbazole moiety of **3**, which can also be clarified by the spectrum of **1** (Fig. S23). As for the peak at 465 nm, it should result either from intramolecular stacked 2,7-dimethoxylcarbazole moiety of 1,3-alternate conformation of **3**, or from its intermolecular aggregations, or from both. Dynamic light scattering (DLS) (Fig. S26a in Supporting information) shows that the average diameter of **3** is ~209 nm and polydispersity index (PDI) value is 0.596. Both the large average diameter and the poor PDI value indicate that **3** exists in non-specific intermolecular aggregated forms, which accounts for its emission peak at 465 nm.

Fig. S26g (Supporting information) shows that berberine alone is not well dispersed either and its average diameter is 1219 nm with PDI of 1.0. However, when **3** is mixed with berberine, the average diameter becomes smaller and PDI becomes better (Figs. S26b–f in Supporting information). The **3**/berbeine complexes at 1/2 molar ratio possess the best PDI (0.209) and the smallest average diameter (~31 nm), as shown in Fig. 4. This result indicates that the **3**/berberine complexes in 1:2 M ratio form a well defined nanometer-sized assembly. In contrast, DLS data (Fig. S27 in Supporting information) shows that the addition of berberine remarkably increases the average diameter of **1** and the PDI value, indicating the existence of precipitation in **1**-berberine non-specific binding system.

Transmission electron microscopy (TEM) images are also recorded (Fig. S28 in Supporting information). Neither free berberine nor free **3** exhibits a well defined morphology. However, **3**/berberine (1:2) complexes generate a highly dispersed nanoparticle (Fig. 4b). Two major morphologies are observed, one is hollow sphere-like structure and the other is solid rodlike (or ellipse) particle. The latter one is the dominated structure within the field of vision. Based on TEM image of **3**/berberine complexes, the determined diameter of spherical aggregates is around 32 nm; the length (long axis) and width (short axis) of rod-like particle are ~47 nm, ~28 nm, respectively, consisting with the results of the above-mentioned DLS experiments. As a control, the **1**/berberine complexes simply present the large particle (Fig. S29 in Supporting information).

In order to further understand the interaction ratio between **3** and berberine, we recorded UV–vis spectra of berberine upon addition of **3** (Fig. S30 in Supporting information). In this way of titration, the absorbance of berberine at ~420 nm is not overlapped with that of **3** (Fig. S22), the association constant can be accurately calculated because of the excluded interference from overlapped spectra. Jobs plot clarifies the 1:2 binding stoichiometry of **3**/berberine (Fig. S31 in Supporting information). A_{475nm} in Fig. S30 is used as y-axis to plot a curve as a function of [**3**], which is listed in Fig. S32 (Supporting information). The curve can be fitted well using a 1:2 model [45], which gives the association constant of 1.2×10^8 $(mol/L)^{-2}$ with a satisfactory R^2 value (0.9884). Subsequently, UV–vis spectra of berberine upon addition of the control compound **1** are recorded and it can be seen that **1** does not affect the absorption spectrum of berberine (Fig. S33 in Supporting information).

To further illustrate the binding nature, ^{1}H NMR of berberine was recorded upon addition of **3**. Fig. 5 shows that addition of **3** makes H_a, H_b, H_c, H_d and H_e of berberine shift upfield, while the other protons remain unaffected (Fig. S34 in Supporting information). It indicates that only one side of berberine is shielded by the carbazole moiety of **3**. When more **3** is added ([**3**]/[berberine] > 0.5), the solution in NMR tube becomes cloudy and the signals of protons of berberine become broad, due possibly to production of the large size particles or precipitation. As such, we cannot obtain an informative NOESY and have to resort to our previous knowledge to gain more insight of their possible binding pattern. Calix[4]carbazole often possesses 1,3-alternate conformation and behaves like a two perpendicular molecular tweezer [37,40,41], which is also clarified by a molecular model in Fig. S35 (Supporting information). Considering the 1:2 host/guest binding ratio resulted from UV–vis, DLS and TEM experiments, the most possible binding pattern would be that one molecule of **3** clamps two molecules of berberine by its two perpendicular molecular tweezers. As such, the host-guest complexes possess the two hydrophilic ammonium carboxylates head groups and the hydrophobic carbazole moieties in between two hydrophilic head groups. So, the host-guest complexes can be considered as an amphiphilic molecule, and thus self-assembling to become nanoparticles (Fig. 6). As for the existence of the rodlike (ellipse) nanoparticle, we propose that it may experience a process of sphere vesicles - necklace like - rodlike structures, proposed by Huang *et al.* [46].

As we know, an ideal sensor should possess a low toxicity. If it can help to reduce the toxicity of berberine, such a sensor would be more valuable.

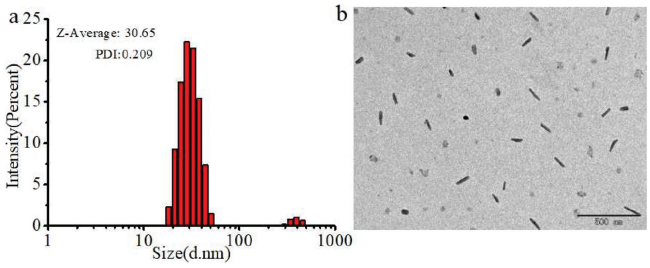

Fig. 4. (a) DLS size distribution of berberine + **3** (molar ratio = 2/1); (b) TEM image of lyophilized sample of berberine + **3** (molar ratio = 2/1).

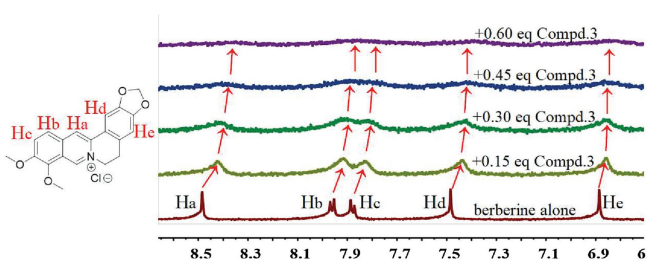

Fig. 5. Partial ^{1}H NMR spectra of berberine (2 mmol/L) upon addition of **3** in D_2O containing 40% DMSO-d_6.

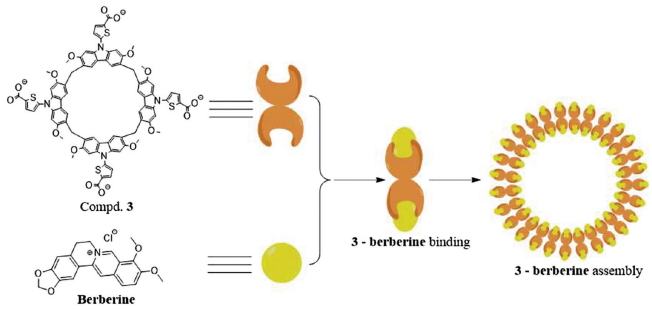

Fig. 6. The possible assembling mode.

To examine these properties of **3**, we measured the toxicities of the free berberine, the free **3** as well the **3**-berberine complexes, respectively, towards the human liver normal cell L02. As IC_{50} value cannot be measured accurately because cell growth is inhibited by berberine at relatively high concentration, where it begins to precipitate. We simply present the cell viabilities to show the toxicity of **3** and its berberine-detoxicating property.

Fig. 7 shows that the cell viabilities of **3** at 75 μmol/L and at 100 μmol/L are 84% and 78%, respectively, which indicates its low toxicity. The cell viabilities of the 1:2 complexes of **3**/berberine at 75/150 μmol/L and at 100/200 μmol/L are 89% and 85%, respectively, which are higher than that of both the free **3** and the free berberine. These results definitely illustrate that **3** not only possesses a low toxicity but also can reduce the toxicity of berberine towards L02 cell.

As for the reason why **3** can reduce the toxicity of berberine, we propose that its acid structure accounts for it. **3** possesses the sodium carboxylates head groups, which makes it soluble in water at neutral pH. This feature would make it retain berberine at neutral pH, which is in agreement with the fact that the normal cells survive more, due to the fewer drugs cellular uptake.

On the other hand, under acid condition, the sodium carboxylates head groups of **3** will be protonated, which will decrease its solubility in water. This feature may make it release drugs under acid condition, which is usually the characteristic micro-environment of some diseases such as tumor and inflammatory cells/tissues. To verify this surmise, we measured the berberine-releasing property of **3** under acid condition. The DLS, fluorescence and TEM of **3**/berberine complexes under acid condition have been examined. Fig. 8a presents that at pH 5.5, the average diameter of host-guest assembled system becomes

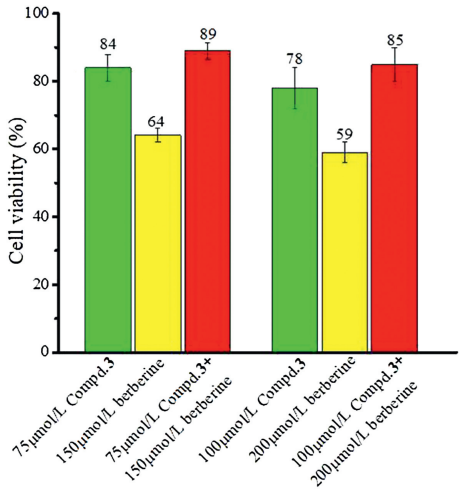

Fig. 7. Viability of L02 cell treated with free berberine, free **3** and the **3**-berberine complexes 48 h at different concentrations.

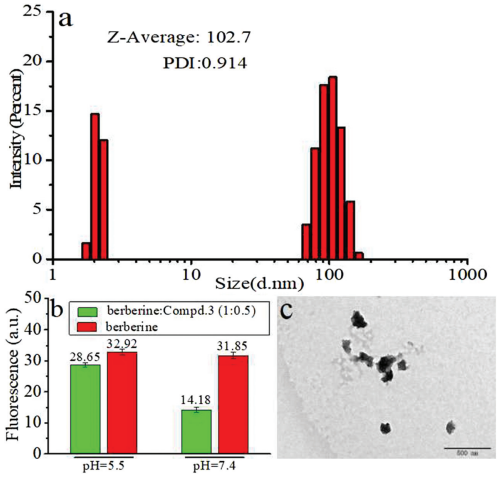

Fig. 8. (a) DLS size distribution of berberine + **3** (molar ratio = 2/1) in pH 5.5 PBS buffer. (b) Fluorescence of berberine and **3**-berberine complexes in different pH buffer. (c) TEM of **3**-berberine complexes in pH 5.5 PBS buffer.

larger (~103 nm) and PDI turns to be worse (0.914); Fig. 8b shows that fluorescence intensity of host-guest complexes is higher at pH 5.5 than that at pH 7.4. TEM image in Fig. 8c shows that at pH 5.5, the original well-defined nanoparticles become poorly dispersed pieces. The above results indicate that the encapsulated berberine is released under acid condition. The calculated drug-loading rate and the releasing rate are 33%, 77% respectively.

We further measured the release of berberine to cells under acid condition. As shown in Fig. 8b, when berberine is released, its fluorescence turns on. This property could be used to stain the cells. As HepG2 cells often generate acid micro-environment, we then use it as the model disease cell. HepG2 cells are then treated with drugs for 10 h either in pH 7.4 buffer or in pH 5.5 buffer. Cells are subsequently washed, visualized by fluorescence confocal microscopy to determine the cell uptake efficiency (Fig. S36 in Supporting information). The normalized result in Fig. S35b shows that at neutral micro-environment, the **3**/berberine complexes are uptaken less than the free berberine. In contrast, at pH 5.5, the **3**/berberine complexes are uptake by HepG2 as efficiently as the free berberine does. This result further confirms that berberine is retained in pH 7.4 buffer, but is released under acid condition. Moreover, **3** does not affect the mitochondrion-targeting feature of berberine (Fig. S37 in Supporting information).

In the end, in order to learn our sensor's relative merits, the properties of some other reported fluorescent sensors have been listed in Table S1 (Supporting information). It could be seen that most of them possess the excellent selectivity and sensitivity, and that different sensors have their own advantages and disadvantages. However, as shown in Table S1, molecular sensors are relatively less than the material-based sensors and the ratiometric sensor for berberine is rarer. Moreover, fewer sensors' cell toxicity has been reported. As such, our macrocyclic probe is advantageous in its fluorescence turn-on and ratiometric detection of berberine, a low toxicity as well as its detoxicating property for this drug.

In conclusion, we recently synthesized a thiophenecarboxylic acid derived calix[4]carbazole (**3**) and determined its drug-sensing property. This macrocyclic probe can not only specifically and ratiometrically detect berberine, but also reduce berberine's toxicity to human normal L02 cell lines. The reason is that **3** is able to be co-assembled with berberine to form well-defined particles. Furthermore, **3** neither retard berberine' release to the tumor cells and nor change its mitochondrion-targeting feature. Therefore, **3** is a low toxic, turn-on and ratiometric sensor capable of detoxicating berberine.

Declaration of competing interest

The authors report no declarations of interest.

Acknowledgment

We thank the Natural Science Foundation of Liaoning Province (No. 20180550874).

Appendix A. Supplementary data

Supplementary material related to this article can be found, in the online version, at doi:https://doi.org/10.1016/j.cclet.2020.10.048.

References

[1] A.H. Amin, T.V. Subbaiah, K.M. Abbasi, Can. J. Microbiol. 15 (1969) 1067–1076.
[2] M. Ikram, Planta Med. 28 (1975) 353–358.
[3] C.L. Kuo, C.W. Chi, T.Y. Liu, Cancer Lett. 203 (2004) 127–137.
[4] K.C. Huang, W.M. Williams, The Pharmacology of Chinese Herbs, 2nd ed., CRC Press, New York, 1999, pp. 381–383.
[5] W. Kong, J. Wei, P. Abidi, et al., Nat. Med. 10 (2004) 1344–1351.
[6] H.H. Guo, C.L. Feng, W.X. Zhang, et al., Nat. Commun. 10 (2019) 1981.
[7] M. Imenshahidi, H. Hosseinzadeh, Phytother. Res. 30 (2016) 1745–1764.
[8] M.M. Kheir, Y. Wang, L. Hua, et al., Food Chem. Toxicol. 48 (2010) 1105–1110.
[9] K. Kummerer, Chemosphere 75 (2009) 417–434.
[10] Y. Linn, J. Lu, L. Lim, et al., Phytother. Res. 26 (2012) 682–686.
[11] A.F. Cicero, A. Ferroni, S. Ertek, Expert Opin. Drug Saf. 11 (2012) 753–766.
[12] W. Chen, Y.Q. Miao, D.J. Fan, et al., AAPS PharmSciTech 12 (2011) 705–711.
[13] L. Liu, Z. Chen, Anal. Chim. Acta 737 (2012) 99–104.
[14] W.Y. Hua, L. Ding, Y. Chen, et al., J. Pharm. Biomed. Anal. 44 (2007) 931–937.
[15] A. Geto, M. Pita, A.L. De Lacey, et al., Sens. Actuators B: Chem. 183 (2013) 96–101.
[16] X.B. Pang, C.Z. Huang, J. Pharm. Biomed. Anal. 35 (2004) 185–191.
[17] J. Xiong, L. Yang, L.X. Gao, Anal. Bioanal. Chem. 411 (2019) 5963–5973.
[18] A. Wen, X. Peng, P. Zhang, et al., Anal. Bioanal. Chem. 410 (2018) 6489–6495.
[19] M. Cao, M. Liu, C. Cao, et al., Spectrochim. Acta Part A 75 (2010) 1043–1046.
[20] J. Ling, Y. Sang, C.Z. Huang, J. Pharm. Biomed. Anal. 47 (2008) 860–864.
[21] Y. Yang, X. Yang, C.X. Jiao, et al., Anal. Chim. Acta 513 (2004) 385–392.
[22] Y. Wu, Q. Zhang, Y. Zhao, et al., ACS Sustain. Chem. Eng. 8 (2020) 6517-6523.
[23] L. Bai, H. Yao, L. Yang, et al., Chin. Chem. Lett. 30 (2019) 881–884.
[24] G. Huang, W. Liu, A. Valkonen, et al., Chin. Chem. Lett. 29 (2018) 91–94.
[25] Z. Laughrey, B.C. Gibb, Chem. Soc. Rev. 40 (2011) 363–386.
[26] J. Murray, K. Kim, T. Ogoshi, et al., Chem. Soc. Rev. 46 (2017) 2479–2496.
[27] F. Jia, H. Hupatz, L.P. Yang, et al., J. Am. Chem. Soc. 141 (2019) 4468–4473.
[28] Y.F. Ding, J. Wei, S. Li, et al., ACS Appl. Mater. Interfaces 11 (2019) 28665–28670.
[29] Y. Li, H. Wu, L. Du, Chin. Chem. Lett. 20 (2009) 322–325.
[30] M. Megyesi, L. Biczók, I. Jablonkai, J. Phys. Chem. C 112 (2008) 3410–3416.
[31] Z. Miskolczy, L. Biczók, J. Phys. Chem. B 118 (2014) 2499–2505.
[32] X. Zhang, X. Wang, B. Wang, et al., Chin. Chem. Lett. 31 (2020) 3230-3232.
[33] Y. Zhang, Y.L. Cui, L.N. Gao, et al., Int. J. Biol. Macromol. 59 (2013) 363–371.
[34] D. Mao, Y. Liang, Y. Liu, et al., Angew. Chem. Int. Ed. 56 (2017) 12614–12618.
[35] M. Guo, W. Li, Y. Sun, et al., Luminescence 34 (2019) 558–562.
[36] P. Yang, Y. Jian, X. Zhou, et al., J. Org. Chem. 81 (2016) 2974–2980.
[37] G. Li, L. Zhao, P. Yang, et al., Anal. Chem. 88 (2016) 10751–10756.
[38] Z. Shu, Y. Chen, H. Yu, et al., Chem. Commun. 55 (2019) 5491–5494.
[39] Z.Z. Yang, Y. Chen, G. Li, et al., Chem. Eur. J. 24 (2018) 6087–6093.
[40] L. Zhao, L. Kang, Y. Chen, et al., Spectrochim. Acta Part A 193 (2018) 276–282.
[41] S. Li, S. Ji, L. Zhao, et al., Chin. J. Org. Chem. 39 (2019) 2860–2866.
[42] X. Liao, W. Guo, J. Zhang, et al., Org. Chem. Front. 7 (2020) 2291–2297.
[43] Y. Yan, X. Zhang, X. Zhang, et al., Chin. Chem. Lett. 31 (2020) 1091–1094.
[44] H.U. Kim, J.H. Jang, F. Xu, et al., J. Nanosci. Nanotechnol. 16 (2016) 2773–2778.
[45] P. Thordarson, Chem. Soc. Rev. 40 (2011) 1305–1323.
[46] Y. Yao, M. Xue, J. Chen, et al., J. Am. Chem. Soc. 134 (2012) 15712–15715.